Modeling and analysis of mixed flow of cars and powered two wheeelers

Sosina M. Gashaw[1]
EURECOM, Campus SophiaTech,
06904 Biot Sophia Antipolis,
phone: +33 (0)4 93 00 82 19,
gashaw@eurecom.fr

Paola Goatin
Inria Sophia Antipolis - Méditerranée,
06902 Sophia Antipolis Cedex,
phone: +33 (0)4 92 38 78 34,
paola.goatin@inria.fr

Jérôme Härri
EURECOM, Campus SophiaTech,
06904 Biot Sophia Antipolis,
phone: +33 (0)4 93 00 81 34,
Jerome.Haerri@eurecom.fr

5186 words + 6 figures + 3 table $\Rightarrow$ 7436 'words'

[1]Corresponding author

Abstract

In modern cities, a gradual increase of motorcycles and other types of Powered Two-Wheelers (PTW) are observed as an answer to long commuting in traffic jams and complex urban navigation. Such increasing penetration of PTW creates mixed traffic flow conditions with unique characteristics that are not well understood. Unlike cars, PTWs filter between cars, have unique dynamics, and do not respect lanes discipline, therefore requiring a different modeling approach than traditional 'Passenger Car Equivalent' or 'Follow the Leader'. Instead, this work proposes to model the flow of PTWs similarly to a fluid in a porous medium, where PTWs 'percolate' between cars as function of the gap between them. Our contributions are as follows: (I) a characterization of the distribution of the gap between vehicles by the densities of PTWs and cars; (II) a definition of the equilibrium speed of each class as a function of the densities of PTWs and cars; (III) an impact analysis of the gradual penetration of PTWs on cars and on heterogeneous traffic flow characteristics.

keyword Multiclass traffic flow model; Motorcycle; PTW; Porous flow; Traffic impacts analysis

Table of symbols

Symbol	Meaning
PTW	Powered Two Wheelers
x	spatial location
t	time
$q_{1/2}$	flow of PTWs/cars
$\rho_{1/2}$	density of PTWs/cars
$v_{1/2}$	speed of PTWs/cars
$v_{1/2}{}^f$	free flow speed of PTWs/cars
i	vehicle class
R	radius of circle
l_p	length of Delaunay edge for points
l_c	length of Delaunay edge for circles

TABLE 1: Table of Symbols And Acronym Used Along The Paper

1   Introduction

While a car is seen as a social achievement in most of the eastern countries, drivers in Europe slowly replace them with motorcycles and other types of Powered Two-Wheeler (PTW) to mitigate their perceived impact of traffic congestion (e.g. reduced travel time). In some cities, electrical scooter sharing initiatives are also proposed for drivers to switch transportation modes when reaching city centers. Yet, PTWs create traffic flow effects (e.g. car flow reduction in presence of PTWs, PTW filtering between and up car streams, etc..) that are difficult to understand with the current available models. Without such understanding, it is difficult to evaluate or develop innovative transportation solutions with or for PTWs, such as adapting traffic lights to PTWs, safety-related PTW applications such as collision/approach warnings, or multi-modal initiatives.

The interaction between PTWs and cars creates mixed traffic flow situations, for which state-of-art models are not adapted. Multi-class flow modeling arises as an effort to characterize such mixed traffic flow situations, which may be characterized roughly in two domains: Mixed 'driver' characteristics or mixed 'vehicle' characteristics. We focus in this work on the latter case, where a classification among the vehicle classes is made on lane specific patterns, vehicles physical and dynamical features [1], and where each vehicle in a class possesses identical characteristics [2].

Multi-class traffic flows are usually evaluated following a metric called "Passenger Car Equivalent" (PCE), which reports the impact of one class of traffic on traffic flow variables. With PCE a heterogeneous traffic flow is converted to a hypothetical homogeneous flow by representing the influence of each vehicle in terms of the equivalent passenger car. PCE value for vehicles varies with the traffic conditions [3] and the value is selected depending on traffic speed, headway and other traffic variables [4]. Although used as a reference metric by the Highway Capacity Manual, it is not adapted to situation, where one class of traffic has significantly different properties (ex. trucks and cars), or when lane discipline and car following are not respected, which is exactly the case with PTWs.

Multi-class models use different approaches to characterize heterogeneous traffic flow. For instance, the multi-class model in [5] extends LWR model for heterogeneous drivers by distinguishing the vehicle classes by the choice of speed. The assumption is that drivers respond in a different way to the same traffic density. A two-classes flow model proposed in [6] differentiates vehicles according to their length and speed. Despite providing a separate representation for each vehicles classes, both classes have the same critical and jam density values, as well as a common speed in congestion regime. The model in [7] [8] formulate a mixed flow of passenger cars and trucks based on their free flow speed difference. In this model, the classification is aimed only to determine collective flow characteristics. Similarly, the work in [9] presents a mixed flow for several populations of vehicles, where the vehicle classes are differentiated on the maximal speed, expressed as function of total occupied space. The model in [10] uses a similar approach as in [9], yet integrating a specific maximum occupied space for each vehicle class.

Mixed flows consisting of PTWs yet exhibit distinctive features from the assumption taken in the previously described multi-class models, making them look more like disordered flows without any lane rule. Their narrow width indeed grants PTWs flexibility to share lanes with other vehicles or filter through slow moving or stationary traffic, requiring traffic stream attributes to be defined differently from traffic following lane rules [11]. Accordingly, Nair and Mahmassani [12] proposed to model PTWs as a fluid passing through a porous medium. The speed-density relationship is presented in terms of pore size distributions, which Nair and Mahmassani obtained through

exhaustive empirical simulations. This approach is computational very expensive and hardly re-producible, as it requires different set up for each scenario being considered. On a later work from the same authors [13], the pore size distribution is assumed to follow an exponential distribution. Yet, a justification for this choice of distribution, as well as its parameters are not given, restricting this work to the modeling of uncorrelated free flow traffic situations.

This paper focuses specifically on a more realistic modeling of the pore size distribution, which is critical to mixed flow models based on a porous medium strategy. Our first contribution provides an enhanced mixed flow modeling called *Porous G*, for which we: (i) provide a close form formula for the pore size distribution for generic traffic flow consisting of cars and PTWs; (ii) propose a mathematical formulation for the fundamental relation of density and speed for both cars and PTWs; (iii) apply a consistent discretization method for the approximation of the conservation equations. Our second contribution evaluates the impact of our proposed *Porous G* model to traffic flow characteristics, where we: (i) evaluate the impact of the maximum road capacity; (ii) formulate mixed flow travel time, and this considering a gradual increase of PTWs.

2 Model description

One of the approaches in macroscopic modeling is the first order model developed by LWR [14, 15]. In LWR model traffic flow is assumed to be analogous to a one directional fluid motion where macroscopic traffic state variables are described as function of space and time. Mass conservation law and the fundamental relationship of macroscopic state variables, namely, speed, density, and flow are the basic elements for LWR formulation. The conservation law says that with no entering or leaving vehicles the number of vehicles between any two points is conserved. Thus, first order PDE equation based on the conservation law takes the form:

$$\frac{\partial \rho(x,t)}{\partial t} + \frac{\partial q(x,t)}{\partial x} = 0 \tag{1}$$

where $\rho(x,t), q(x,t)$ are respectively the density and the flow of cars at position x and time t. Flow $q(x,t)$ is expressed as function of traffic state variables.

$$q(x,t) = \rho(x,t)v(x,t) \tag{2}$$

The speed $v(x,t)$ depends on density and a unique speed value corresponds to a specific traffic density, i.e.

$$v(x,t) = V(\rho(x,t))$$

The assumption on equilibrium speed-density relation implies that vehicles instantaneously adapt to the speed value corresponding to the density at their position, which is one of the limitations of LWR models.

In the original LWR model, all vehicles in a traffic stream are considered to exhibit similar characteristics, thus, no classification is made between vehicle classes. Multi-class extension of LWR model emerge to accommodate the heterogeneity in many aspects of road users. In multi-class modeling vehicles with identical characteristics are grouped into a class and a conservation law applies to each class. Our interest here is in modeling traffic flow consisting of cars and PTWs

and we start by formulating conservation equation for two classes of vehicles.

$$\frac{\partial \rho_i(x,t)}{\partial t} + \frac{\partial q_i(x,t)}{\partial x} = 0 \qquad i = 1,2 \tag{3}$$

Where ρ_i and q_i denote density and flow of class i, respectively. Class specific flow, speed and density are related by equation:

$$q_i(x,t) = \rho_i(x,t)v_i(x,t) \qquad i = 1,2 \tag{4}$$

Since both vehicle classes share the same road space, the flow of a given vehicle class not only depends on the number of vehicles in the same class but also on the number of vehicle from the other class. Hence, the equilibrium speed v_i for individual vehicle class i is a function of the densities of both classes and satisfies the following conditions:

$$v_i = V_i(\rho_1, \rho_2), \qquad \partial_1 V_i(\rho_1, \rho_2) \le 0, \ \partial_2 V_i(\rho_1, \rho_2) \le 0. \tag{5}$$
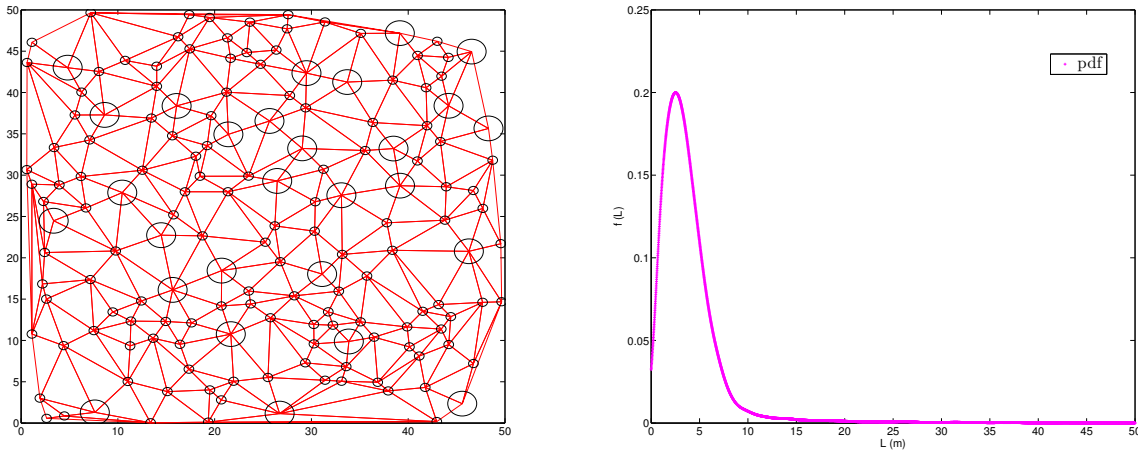
The interaction among vehicle classes is captured through the equilibrium speed. To formulate the speed of each class as a function of the two densities, which is also equivalent to total density and traffic composition, we begin first by analyzing underlying behaviors in mixed flow of cars and PTWs. In light traffic situations, there is pretty few interaction among the two classes. Therefore, they freely travel at speed close to their maximum speed. For higher traffic levels, however, the presence of one vehicle class affects others and each class responds to the situation differently. PTWs are associated with unique behaviors such as they can share a lane with other vehicles, filter between lanes of traffic, keep small clearance with other vehicles, filter through stationary cars. Due to these capabilities, PTWs can move at higher speed than cars.

According to the above explanation, PTWs tend not to follow lane rules. Thus, we approximate the flow of cars and PTWs mix with a nonlane based traffic flow where all vehicles use available gaps between other vehicles to move forward, which is similar to the flow of a fluid through a porous medium [12]. Adapting the concept to traffic flow, we can say that vehicles maneuver through available free spaces along the way. In traffic mix of cars and PTWs, due to the vehicles size difference a space that can admit PTWs may not be enough for cars. Accordingly, the speed of vehicles determined by dynamics and physical properties plus the availability of enough free space for that vehicle class. Free space distribution, on the other hand, depends on a number of vehicles and traffic composition. This implies that representing vehicles speed as a function of free space (pore) is equivalent to expressing the speed as a function of the number and the composition of vehicles. To complete the formulation of speed function, the distribution of gap between vehicles or pore size is required. The next part addresses vehicle spacing distribution.

2.1   Vehicle spacing distribution

For the sake of simplicity, we take the following assumptions: cars and PWTs have circular shape and they are distributed in the domain uniformly and independently according to Poisson point process with intensity λ, where λ is number of vehicles per unit area. Furthermore, Delaunay triangulation is used to define the spacing between vehicles on the assumption that Delaunay triangle edge length represents size of the spacing.

Given the density of each vehicle classes, vehicles are placed uniformly and independently without overlapping in a two-dimensional finite space with intensity $\lambda = \rho_1 + \rho_2$. Here, ρ_1 and ρ_2 represent PTWs and cars areal density respectively. Delaunay triangulation constructed over the center of vehicles (Figure 1(a)) and triangles edge length data from 30 simulation runs is used to estimate the probability density function. Once the estimated probability density function is known, by employing Matlab curve fitting tool a standard distribution that gives a good approximation is selected. The comparison between distribution function is based on the statistics on R-square, sum of squared errors (SSE) and root mean square error (RMSE) values.

(a) Delaunay triangulation over vehicles.

(b) Probability density function.

FIGURE 1: Pore size distribution example for $\rho_1 = 0.05, \rho_2 = 0.01 veh/m_2$.

Based on the comparison outcome, Gaussian distribution conforms better to the estimated PDF than other distributions. We consider

$$f_p = \frac{1}{\sqrt{2\pi}\sigma} \exp \frac{-(x-\mu)^2}{2\sigma^2} \tag{6}$$

where μ is the mean pore size and σ is the standard deviation. Yet, the mean pore size and standard deviation are unknown. In [16] it is indicated that for a Delaunay triangulation performed on homogeneous planar Poisson point with intensity λ the mean values for the length of Delaunay triangle edge and square of the length is given by $E(l_p) = \frac{32}{9\pi\sqrt{\lambda}}$ and $E(l_p^2) = \frac{5}{\pi\lambda}$, respectively. Starting from this we can formulate for the case of circles. We have two type of circles, small circles for PTWs and large circles for cars. When points replaced by circles, edge length measured for points is reduced by the sum of radius of the circles the two end points of the edge connected to. For instance, an edge connecting PTWs and cars reduced by $R_1 + R_2$, where R_1 and R_2 are radius of a circle representing PTW and car respectively. Confirming with average of Delaunay age length for points, for circles it can be defined as:

$$E[l_c] = E[l_p] - 2(R_1 p_1 + R_2 p_2)$$

p_1 is probability for an edge to touch PTWs and p_2 for cars. This probability is expressed in the

form $p_i = \frac{\rho_i}{\rho_1 + \rho_2}$.

$$E(l_c) = \mu = \frac{32}{9\pi\sqrt{\rho_1 + \rho_2}} - \frac{2(R_1\rho_1 + R_2\rho_2)}{\rho_1 + \rho_2}$$

Standard deviation and variance are the same for the case of points (σ_p^2) and circles(σ_c^2), thus

$$\sigma_p^2 = E(L_p^2) - E(L_p)^2 \approx \frac{3}{\pi^2\lambda} \qquad\qquad \sigma_c^2 = \frac{3}{\pi^2(\rho_1 + \rho_2)}$$
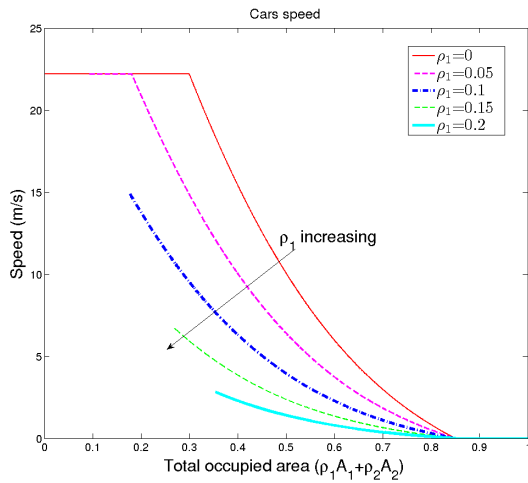
Since the pore size value always takes positive values we use left truncated Gaussian distribution i.e.

$$f_{pTN}(l) = \begin{cases} 0 & l < 0 \\ \frac{f_p(l)}{\int_0^\infty f_p(l)} & l \geq 0 \end{cases} \tag{7}$$
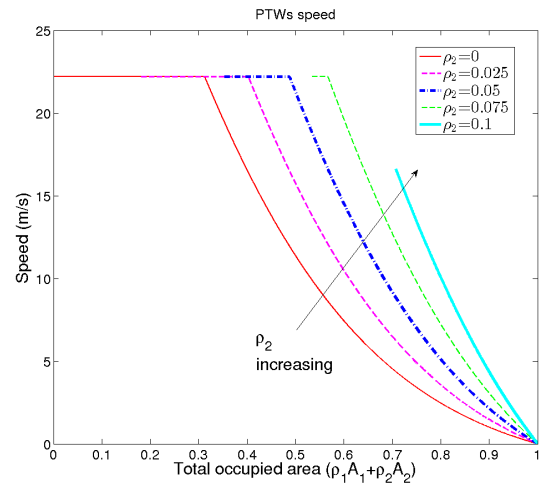
The speed function that computes the average speed for each class is formulated based on the following assumptions. Each vehicles class has associated critical pore width r_i^c, which is the minimum pore width that allows a vehicle to pass through. Two group of vehicles exist in a given vehicle class, vehicles moving or vehicles stopped because of not finding enough space to progress forward. The portion of vehicles moving is proportional to the fraction of pore space that admits a given vehicle class. Here, we are also assuming that all vehicles that find a space greater than to the critical pore size move at the same speed, i.e free flow speed v_i^f. In accordance with the above hypothesis, the average speed for each class is formulated as:

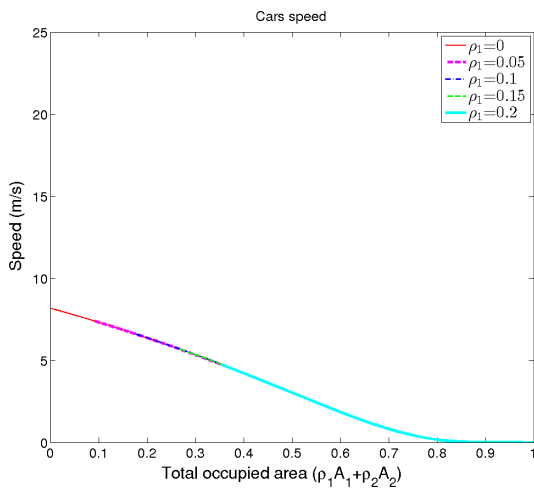$$v_i = v_i^f \left(1 - \int_0^{r_i^c} f_{pTN}(l)\, dl\right) \tag{8}$$

where v_i^f is the free flow speed of class i. In this formulation (Eq. 8), the speed value never becomes zero, which is a limitation. For this, normalization of speed is applied as a countermeasure. We have selected different jam area occupancy for the two classes and the speed values are normalized so that its value becomes zero at the jam area occupancy. Jam area occupancy, i.e. $\rho_1 a_1 + \rho_2 a_2$, is set to 1 for PTWs and to 0.85 for cars.
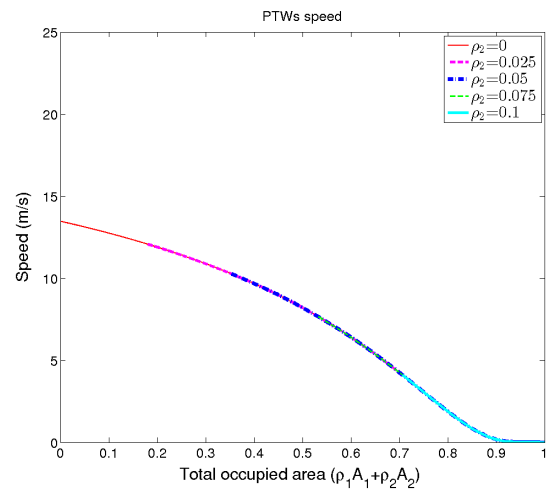
(a) Car speed - *Porous G.*

(b) PTWs speed - *Porous G.*

(c) Car speed - *Porous exponential.*

(d) PTW speed - *Porous exponential.*

FIGURE 2: Car and PTW speed as function of the total occupied area, considering different density values of PTW and cars, respectively.

A further modification is applied to the speed function in order to comply with two phase Macroscopic fundamental diagrams theory. In two phase macroscopic fundamental diagram there exist a free flow and congestion regimes. In free flow there is no significant drop of average speed with increase of density. However beyond the maximum density for the free flow, the average speed of vehicles decreases with density increase. We thus set

$$v_1 = \min \left\{ v_1{}^f, C_v v_1^f \left(1 - \frac{1}{N_1} \int_0^{r_1^c} f_{pTN}(l)\, \mathrm{d}l \right) \right\}, \tag{9}$$

$$v_2 = \min \left\{ v_c{}^f, C_v v_2^f \left(1 - \frac{1}{N_2} \int_0^{r_2^c} f_{pTN}(l)\, \mathrm{d}l \right) \right\}, \tag{10}$$

where N_i is a speed normalization factor and C_v is a scaling factor so that v_i equals to free flow speed below the critical density in the presence of traffic of vehicle class i only.

From the speed function of our *Porous G* model, we can clearly see in Figure 2(a) that an increase of the ratio of PTWs over cars for the same area occupancy will reduce the speed value of both vehicle classes and the reverse happens with the decrease of PTWs ratio (Figure 2(b)). The speed plots illustrated in Figure 2(c) and Figure 2(d) depict the evolution of the speed of cars, resp. ptw, as modeled by *Porous exponential* [13] which is counter-intuitive, considering for a given area occupancy depending on the proportion of the two classes the speed value varies.The models proposed in [10][9] exhibit similar property. This illustrates the superior modeling of our proposed *Porous G* model, compared to other baseline models.

Summarizing, the speed function of *Porous G.* model enjoys the following properties:

- A unique speed value is associated with a given total density and traffic composition.

- In free flow vehicles move at constant (maximal) speed.

- In congestion, speed decreases with increase of density.

- Speed depends on the densities of the two vehicle classes and their proportion.

- For the same area occupancy (total area occupied by vehicles) the more the share of PTWs is the lower becomes the speed.

- PTWs and cars have different congestion and free flow regimes.

2.2   System Analysis

For the system (3)-(5) to be hyperbolic, the jacobian matrix Dq of $q = (q_1, q_2)$ should be diagonalizable with real eigenvalues. We can prove the hyperbolicity by showing that the system is symmetrizable, i.e. there exists a positive-definite matrix S such that SDq is symmetric, see Benzoni-Gavage and Colombo [9].
Re-writing the coupled system equation in the form:

$$\frac{\partial \rho}{\partial t} + Dq(\rho) \frac{\partial \rho}{\partial x} = 0$$

where

$$\rho = \left[\begin{array}{c} \rho_1 \\ \rho_2 \end{array} \right] \quad and \quad q(\rho) = \left[\begin{array}{c} \rho_1 v_1(\rho) \\ \rho_2 v_2(\rho) \end{array} \right],$$

the Jacobian matrix of $q(\rho)$ is given by:

$$Dq(\rho) = \left[\begin{array}{cc} \frac{\partial(\rho_1 v_1)}{\partial \rho_1} & \frac{\partial(\rho_1 v_1)}{\partial \rho_2} \\ \\ \frac{\partial(\rho_2 v_2)}{\partial \rho_2} & \frac{\partial(\rho_2 v_2)}{\partial \rho_1} \end{array} \right] = \left[\begin{array}{cc} \rho_1 \partial_1(v_1) + v_1 & \rho_1 \partial_2(v_1) \\ \\ \rho_2 \partial_1(v_2) & \rho_2 \partial_2(v_2) + v_2 \end{array} \right].$$

For $\rho_1 > 0, \rho_2 > 0$,

$$S = \left[\begin{array}{cc} \frac{1}{\rho_1 \partial_2(v_1)} & 0 \\ \\ 0 & \frac{1}{\rho_2 \partial_1(v_2)} \end{array} \right] \tag{11}$$

is a symmetrizer of Dq, thus the system satisfies the hyperbolicity condition.

The eigenvalues of the Jacobian representing information propagation (characteristic) speed are given by:

$$\lambda_{1,2} = \frac{1}{2}[\alpha_1 + \alpha_2 \pm \sqrt{(\alpha_1 - \alpha_2)^2 + 4\rho_1 \rho_2 \partial_2(v_1)\partial_1(v_2)}]$$

where

$$\alpha_1 = \rho_1 \partial_1(v_1) + v_1, \qquad \alpha_2 = \rho_2 \partial_2(v_2) + v_2.$$

Following [9] Proposition 3.1 it is possible to show that

$$\lambda_1 \leq \min\{\alpha_1, \alpha_2\} \leq \min\{v_1, v_2\} \quad and \quad \min\{v_1, v_2\} \leq \lambda_2 \leq \max\{v_1, v_2\},$$

where we have taken $\lambda_1 \leq \lambda_2$. Therefore $\lambda_1, \lambda_2 \leq \max\{v_1, v_2\}$, which confirms that in the model no wave travel at higher speed than the traffic.

2.3   Solution procedure

A finite volume method is applied for the approximation of the conservation laws in Eq. (3). In the approximation, the spatial domain is divided into equal grid cells of size Δx and at each time interval Δt the density value in the domain updated according to the conservation law. Rewriting in the integral form it becomes

$$\frac{d}{dt} \int_{x_{i-1/2}}^{x_{i+1/2}} \rho(x,t)dx = q(\rho(x_{i-1/2}, t)) - q(\rho(x_{i+1/2}, t)) \tag{12}$$

Integrating eq. (12) in time from t^n to $t^{n_1} = t^n + \Delta t$, we have

$$\int_{x_{i-1/2}}^{x_{i+1/2}} \rho(x, t^{n+1})dx = \int_{x_{i-1/2}}^{x_{i+1/2}} \rho(x, t^n)dx$$

$$+ \int_{t^n}^{t^{n+1}} q(\rho(x_{i-1/2}, t))dt - \int_{t^n}^{t^{n+1}} q(\rho(x_{i+1/2}, t))dt. \tag{13}$$

After some rearrangement of Eq. (13), we obtain an equation that relates cell average density ρ_j^n update with average flux values at the cell interfaces.

$$\rho_i^{n+1} = \rho_i^n - \frac{\Delta t}{\Delta x}[F_{i+1/2}^n - F_{i-1/2}^n] \tag{14}$$

where $F_{i+1/2}^n$ is an average flux value at cell interface $x = x_{i+1/2}$ approximated from cell average density values at x_i and x_{i+1}.

$$F_{i+1/2}^n = \mathcal{F}(\rho_i^n, \rho_{i+1}^n) \qquad \text{where } \mathcal{F} \text{ is the numerical flux function.} \tag{15}$$

Accordingly, equation (14) rewrites

$$\rho_i^{n+1} = \rho_i^n - \frac{\Delta t}{\Delta x}[\mathcal{F}(\rho_i^n, \rho_{i+1}^n) - \mathcal{F}(\rho_{i-1}^n, \rho_i^n)]. \tag{16}$$

Our numerical flux function is defined according to the classical LaxFriedrich's scheme [17], which has the form:
$$\mathcal{F}(\rho_i, \rho_{i+1}) = \frac{1}{2}(f(\rho_i) + f(\rho_{i+1})) + \frac{\alpha}{2}(\rho_i - \rho_{i+1}), \tag{17}$$

where α is the numerical viscosity satisfying the condition $\alpha \geq V_{max} = \max\{v_1^f, v_2^f\}$. The spece and time steps Δx, and Δt are selected to meet Courant, Friedrichs and Lewy (CFL) condition, which is a necessary condition for a numerical method to achieve stability and convergence. Therefore, Δt is chosen to satisfy $\Delta t \leq \Delta x / V_{max}$, due to the bounds on the eigenvalues derived in Section 2.2. The choice of the numerical scheme is driven by the lack of information about the system exact solutions, which is required by less diffusive methods like Godunov's scheme.

3 Model verification

In this section, the capability of our model to reproduce observed macroscopic phenomena of mixed flow of PTWs and cars is evaluated. When the traffic volume is high cars start slowing, however, PTWs remain unaffected or less affected by the change in traffic situation as they can ride between traffic lanes. As a consequence, PTWs travel at higher speed and overtake slow moving cars. In addition, when cars are stopped at traffic signals or because of traffic jams, PTWs can find a space to filter (creep) through stationary cars and move ahead. These two well-known features are used as a benchmark to evaluate our model. For creeping and overtaking experiments, the following parameters are chosen.

	PTW	Car
Vehicle length(m)	1.5	3
Vehicle radius(m)	0.75	1.5
Max. speed(m/s)	1.8	1
Jam density porous G.	1	0.85
Jam density creeping	1.8	1
Jam density *N-pop*.	1	1

TABLE 2: Simulation Parameters

Jam density refers to the maximum area occupancy, which equals to $\rho_1 a_1 + \rho_2 a_2$ for *porous G.* model and $\rho_1 l_1 + \rho_2 l_2$ for the other models, where vehicles come to complete stop state. The simulation is done on road length of 50m and $\Delta x = 0.05$ and Δt selected according to CFL condition.

3.1   Creeping experiment

A situation at signalized intersection is employed for testing creeping. In the simulation, PTWs start behind the cars traffic and cars traffic have concentrated close to the traffic signal so that PTWs arrive after most of the cars reached a complete stop. The simulation is done for 200s and start with an initial density of:

$$\rho_1(x,0) = \begin{cases} 0.25 & \text{for } x \in [1,\ 21] \\ 0 & \text{otherwise} \end{cases} \qquad \rho_2(x,0) = \begin{cases} 0.25 & \text{for } x \in [31,\ 50] \\ 0 & \text{otherwise} \end{cases}$$

The inflow and outflow at the boundaries are set to zero. At the time PTWs start catching up cars traffic (Figure 3(a)), most of the cars are at stationary state (see Figure 3(a) lower subplot space location 45-50m). However, as shown in Figure 3(b) PTWs maneuver through those stationary cars and reach to the front of queue for the case of *creeping* and *Porous G.* models. For the *N-pop.* model the PTWs traffic stays behind the cars since both classes have the same jam density.
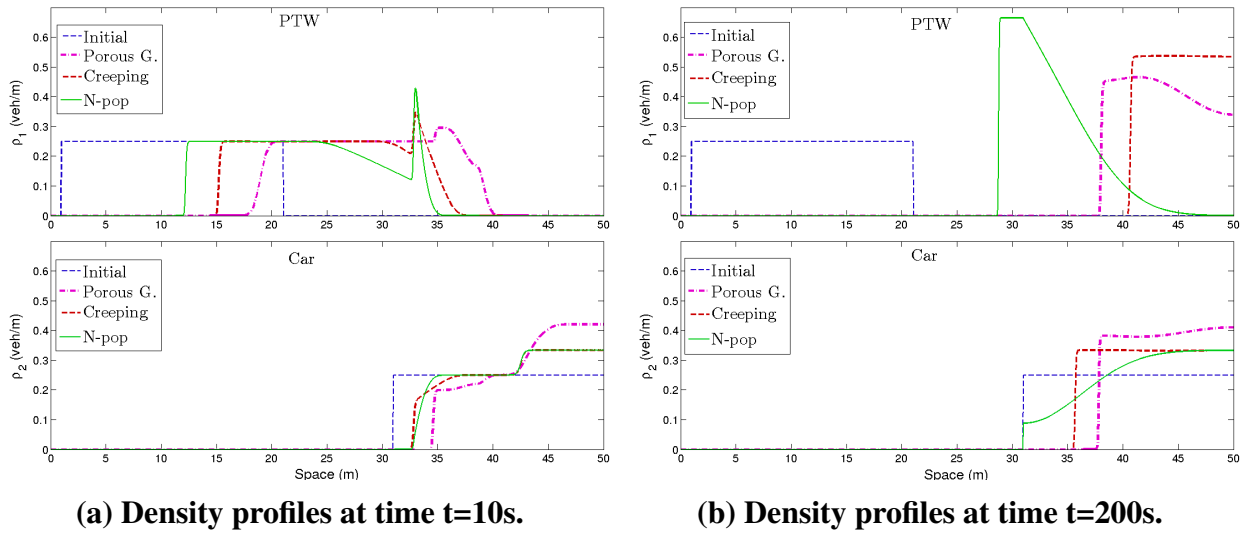
(a) Density profiles at time t=10s.   **(b) Density profiles at time t=200s.**

FIGURE 3: Creeping experiment density-space diagram, upper subplot for PTWs and lower subplot for cars.
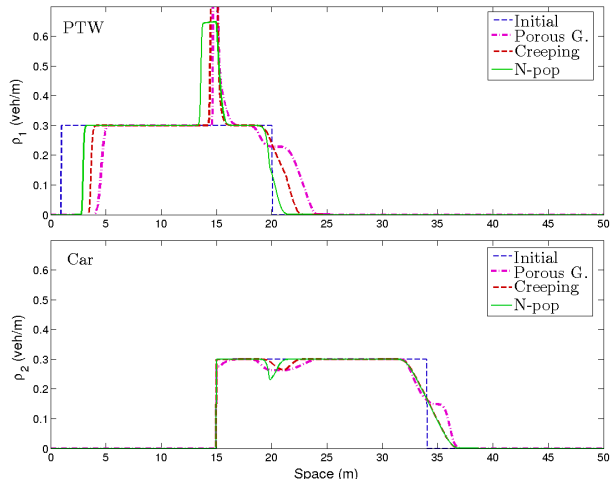
The results from the creeping experiment show similar behavior to the situation we observe in real scenarios, i.e. PTWs seep through cars queue to reach the head the queue, for *Porous G.* and *Creeping* models. However, for *N-pop* model PTWs remain behind car's traffic queue.
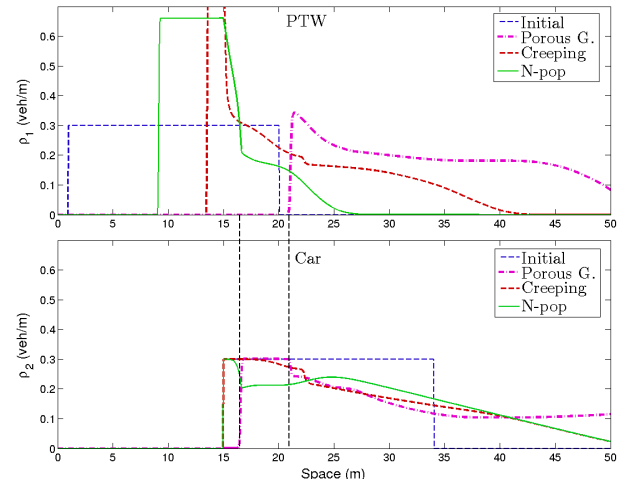
3.2   Overtaking experiment

For the overtaking scenario cars traffic is placed ahead of PTWs. The simulation starts with the initial state where:

$$\rho_1(x,0) = \begin{cases} 0.3 & \text{for } x \in [1,\ 20] \\ 0 & \text{otherwise} \end{cases} \quad \rho_2(x,0) = \begin{cases} 0.3 & \text{for } x \in [15,\ 34] \\ 0 & \text{otherwise} \end{cases}$$
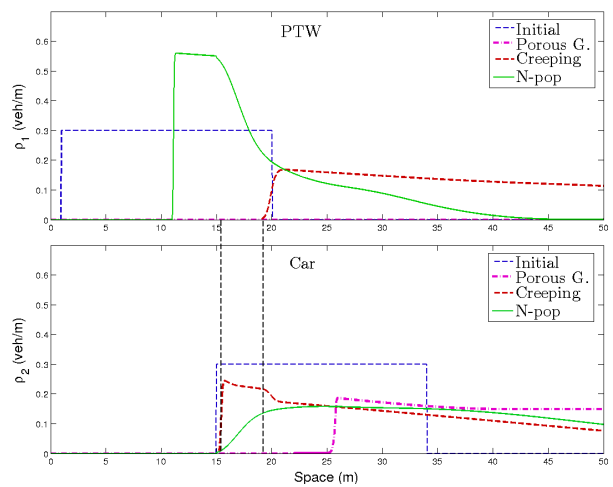
The inflow at upstream boundary is set to zero and vehicles are allowed to leave freely at the downstream boundary. The occurrence of overtaking is evaluated by inspecting the evolution of traffic densities of the two classes. Overtaking is said to happen when the density waves of the two classes come to the same level in space and one of the two go past the other, i.e the tail end of one of the traffics is before the other.
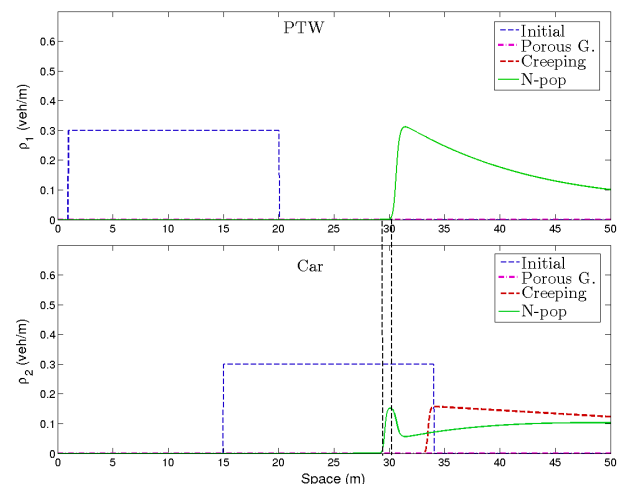
(a) **Density profiles at time t=2sec.**

(b) **at time t=18sec, overtaking in *Porous G*.**

(c) **at time t=38sec, overtaking in *Creeping*.**

(d) **at time t=80sec, overtaking in *N-pop*.**

FIGURE 4: Overtaking experiment density-space diagrams, free flow speed of $V_1 = 1.8m/s$ greater than $V_2 = 1m/s$, upper subplot for PTWs and lower subplots for Car.

As Figure 4 depicts, PTWs overtake cars in all the three models. In *Porous G.* model overtaking is observed around at time t=18sec (4(b)) and for *Creeping* and *N-pop.* models overtaking happens at t=38sec (4(c)) and t=80sec (4(d)), respectively.

According to what is illustrated in the Figure 4, all the three models are able to describe overtaking phenomenon when PTWs free flow speed is higher than cars. Unlike to the two models, in *N-pop* model overtaking never happens unless car free flow speed is higher. The dashed lines stretching from upper subplot to the lower connect the tail of the density profiles for car's and PTWs' traffic. The spacing between the two lines indicates the distance gap after PTWs overtake.

In conclusion, the model verification results validate that our mode (*Porous G.*) can produce the required creeping and overtaking phenomenons. The *Creeping* model also satisfies these properties. However, the model has limitation as occupied space is a mere factor that determines the speed and the variation on the composition of vehicles has no influence as long as the occupied space is the same (see section 2.1 Figure 2).
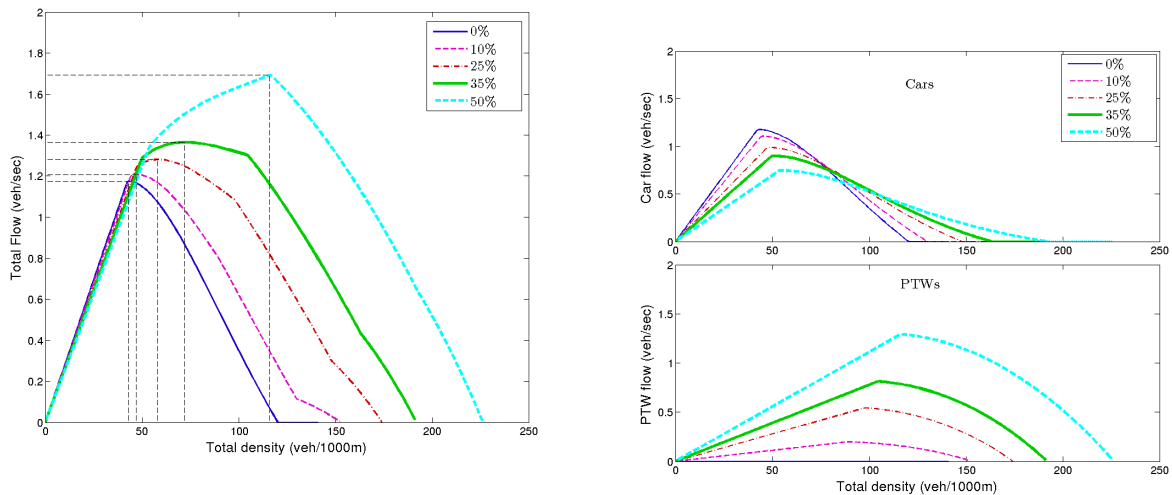
4   Traffic impacts analysis

The section here explores the impact of PTWs on traffic flow, road capacity and queue discharge time. First, the role of PTWs, at different penetration rates, on minimizing congestion is analyzed by substituting some of the cars with PTWs. Following, how shifting travel mode to PTWs could help in the reduction of travel time is investigated.

4.1   Road capacity

Road capacity, which is also called critical density, is defined as the maximum volume of traffic that corresponds to the maximum flow rate. Above the road capacity, traffic flow enters to congestion state and the flow of vehicles decrease with the increase in traffic volume. In mixed traffic flow, the road capacity varies depending on the total density and the traffic composition. Here, the role of PTWs in reducing congestion is evaluated. For the comparison, the flow-density plot for different ratio of PTWs is presented in Figure 5(a).

PTWs stay in free flow state for longer ranges of density than cars because of their ability to ride in between other vehicles. The flow-density diagram, which is depicted by Figure 5(b), shows the variation on maximum flow rate and critical density of the two classes. Figure 5(a) shows the total flow rate against the total volume of vehicles. The total flow rate describes the number of vehicles that leave a given point in a unit time, which is equal to the sum of flow rate of PTWs and cars in our case. As Figure 5(a) illustrates, maximizing the proportion of PTWs on the total traffic from 0% to 10% result in 9.3% improvement on the road capacity and 2.74% on the maximum flow rate. The higher the share of PTWs the better becomes the flow rate.

(a) Total flow rate vs. total density,the connecting dashed lines show the maximum flow rate and the corresponding road capacity.

(b) Flow-total density diagram, upper subplot for cars and lower subplot for cars.

FIGURE 5: Flow-density diagram,for different penetration rates of PTWs.

The result in the Figure 5(a) and the numerical figures in Table 3 signifies that PTWs indeed helps to improve road capacity.

% of PTWs	Critical density (veh/m)	Maximum flow (veh/sec)
0	43.1	1.18
10	47.1	1.2
25	58.1	1.28
35	72.1	1.36
50	116.1	1.69

TABLE 3: The Change in Critical Density and Maximum Flow Rate at Different Ratios of PTWs
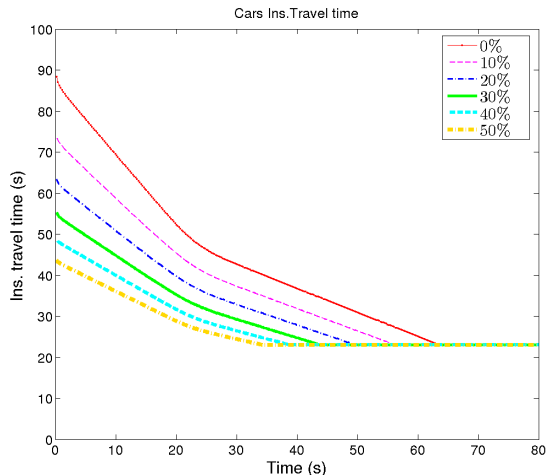
4.2   Travel time

Here, we analysis how replacing some of the cars with PTWs improves travel time. The instantaneous travel time (iTT) is computed on the assumption that vehicles travel through the considered section at a speed profile identical to that of the present local speeds and formulated as:

$$t_{inst} = \sum_{i=1}^{n} \frac{\Delta x}{v(x_i, t)} \tag{18}$$

where n is the number of cells and Δx is the mesh size. The experiment is done on the following simulation setups: road length 500m, Δx=10m, free flow speeds $V_1 = v_2 = 80 km/hr$ and the sim-

ulation is run for 80 sec. A homogeneous initial total density of $\rho_1(x,0) + \rho_2(x,0) = 0.1\ for\ x \in$ $[0,\ 500]$ is set. The result in Figure 6 is produced by computing the instantaneous travel time at each 0.02 sec. According to the result, a 12.4% reduction on average travel time is obtained even at the lowest penetration of PTWs(10%). The numerical figure in the Table are the average iTT values averaged over the whole simulation period. In addition to reduction in average travel time with more shift of cars to PTWs, cars travel at lowest travel time for more duration of the simulation time. Certainly, the results show that PTWs help in maintaining reliable and reduced travel time.

% of PTWs	cars average travel time	Improv. (%)
0	41.6	
10	36.45	12.4
20	32.74	21.3
30	30	27.9
40	28	32.7
50	26.68	35.9

FIGURE 6: Change in travel time of cars for different penetration rate of PTWs.

5   Summary and conclusion

Motorcycle, scooter, and other moped, thereafter referred to as Powered Two-Wheelers (PTW), have peculiar maneuvering behaviors, such as filtering through slow moving or stationary traffic, or lacking lane discipline, which create mixed traffic flow characteristics resembling more disordered flows rather than lane-based follow-the-leader flows. Mixed flow models considering ordered flows accordingly fail to truly represent the impact of PTW on heterogeneous traffic flow characteristics.

This paper specifically investigated a disordered PTW modeling similarly to a fluid in porous medium. An enhanced mixed flow traffic model is provided based on an innovative modeling of the distribution of the space-gap in a porous medium. The space-gap distribution allows us to propose a mathematical formulation of the fundamental relation between speed and density for both cars and PTW individually. This latter aspect could be very beneficial in related traffic flow studies, which assumed identical fundamental relations for PTW or cars.This model is then used to evaluate the impact of a gradual penetration of PTW on mixed flow traffic characteristics. The model has been validated by comparing it against the typical PTW flow characteristics and also benchmarked against related studies.

The evaluation of the impact of PTW on mixed traffic first showed that a gradual penetration manages to increase the flow capacity by 9.3% already with 10% PTW penetration. It also confirmed the benefit of PTW for reducing travel time, but also illustrated the mutual benefit of

a gradual penetration of PTW on travel time of both PTW and passenger cars (12.4 % benefit on cars at 10% penetration of PTW).

The presented model assumes that both classes of vehicles disregard the lane discipline and their spatial distribution over the road segment follows Poisson point process. As a future work, we consolidate the model by applying a more realistic approach for the spatial distribution and lane discipline of cars. Moreover, we consider calibrating the model with empirical data to validate the parameter choices.

Acknowledgment

REFERENCES

[1] F. C. Daganzo, A behavioral theory of multi-lane traffic flow. part i: Long homogeneous freeway sections, Transportation Research Part B: Methodological 36 (2002) 131–158.

[2] S. Logghe, L. H. Immers, Multi-class kinematic wave theory of traffic flow, Transportation Research Part B: Methodological 42 (2008) 523–541.

[3] P. S. Praveen, V. T. Arasan, Influence of traffic mix on pcu value of vehicles under heterogeneous traffic conditions, International Journal of Traffic and Transport Engineering 3 (2013) 302–330.

[4] M. Adnan, Passenger car equivalent factors in heterogenous traffic environment-are we using the right numbers?, Procedia engineering 77 (2014) 106–113.

[5] G. Wong, S. Wong, A multi-class traffic flow model–an extension of lwr model with heterogeneous drivers, Transportation Research Part A: Policy and Practice 36 (2002) 827–841.

[6] S. Chanut, C. Buisson, Macroscopic model and its numerical solution for two-flow mixed traffic with different speeds and lengths, Transportation Research Record: Journal of the Transportation Research Board (2003) 209–219.

[7] H. Zhang, W. Jin, Kinematic wave traffic flow model for mixed traffic, Transportation Research Record: Journal of the Transportation Research Board (2002) 197–204.

[8] J. Van Lint, S. Hoogendoorn, M. Schreuder, Fastlane: New multiclass first-order traffic flow model, Transportation Research Record: Journal of the Transportation Research Board (2008) 177–187.

[9] S. Benzoni-Gavage, R. M. Colombo, An n-populations model for traffic flow, European Journal of Applied Mathematics 14 (2003) 587–612.

[10] S. Fan, D. B. Work, A heterogeneous multiclass traffic flow model with creeping, SIAM Journal on Applied Mathematics 75 (2015) 813–835.

[11] C. Mallikarjuna, K. R. Rao, Area occupancy characteristics of heterogeneous traffic, Transportmetrica 2 (2006) 223–236.

[12] R. Nair, H. S. Mahmassani, E. Miller-Hooks, A porous flow approach to modeling heterogeneous traffic in disordered systems, Transportation Research Part B: Methodological 45 (2011) 1331–1345.

[13] R. Nair, H. S. Mahmassani, E. Miller-Hooks, A porous flow model for disordered heterogeneous traffic streams, in: Transportation Research Board 91st Annual Meeting, 12-3260.

[14] M. Lighthill, G. Whitham, On kinematic waves. i. flood movement in long rivers, in: Proceedings of the Royal Society of London A: Mathematical, Physical and Engineering Sciences, volume 229, The Royal Society, pp. 281–316.

[15] P. I. Richards, Shock waves on the highway, Operations research 4 (1956) 42–51.

[16] R. E. Miles, On the homogeneous planar poisson point process, Mathematical Biosciences 6 (1970) 85–127.

[17] R. J. LeVeque, Numerical methods for conservation laws, volume 132, Springer, 1992.